Hydrodynamic Origin of Whale Flukeprints

Rachel Levy, Dmitri Skjorshammer, John Calambokidis
Harvey Mudd College, Cascadia Research
June 8, 2009

Whales swimming at a shallow depth leave a signature on the ocean surface known as a whale flukeprint. The print is a large, smooth, oval patch surrounded by a small wake or ridge. Informal observations made by biologists have led to hypotheses that the prints are made either by hydrodynamic forces due to the motion of the fluke, or by surfactants, which are surface active agents that lower surface tension. This study employs experiments with an artificial fluke to investigate whether flukeprints can be created by hydrodynamic forces without the presence of surfactant. The effect of swim velocity on the width, length and duration of a flukeprint created by the artificial fluke was analyzed. The experimental data indicate that clear prints can be formed solely by hydrodynamic forces, a conclusion supported by observations of whale researchers and by mathematical modeling proposed for related experiments.

Introduction

Flukeprints are a visible pattern that appears on the surface of the ocean when a whale is swimming nearby (see Fig. 1). Whales swimming at a shallow depth or beginning a terminal dive create a striking oval-shaped patch on the surface of the ocean with small ridges forming the outer circumference and very few capillary (wind-driven) waves in the interior [14, 20, 24]. The patch may remain visible for as long as several minutes, depending on ocean and wind conditions. A popular name for this phenomenon is 'whale footprint' since the prints can be used to track whales over long distances as they migrate. While other swimming animals such as dolphins and manatees create prints on the surface, whales create the largest prints with the longest duration.

The flukeprints are made during two different phases of swimming behavior. One is when the whales are swimming horizontally below the surface. If the whale is swimming this way for a distance, the whales can be tracked by the prints, which occur at fairly regular intervals with each beat of the fluke. The other time prints appear is when the whale is about to make a deep dive. Such "terminal dives" take place after the whale has surfaced for air and after the characteristic sighting of the near-vertical fluke as the whale dives. These prints tend to be larger and are probably the result of the strong thrusts the whales make to dive. Blue whales, which are negatively buoyant, only need to fluke a few times to make a dive. The first of these motions is explored in this paper.

Figure 1: Flukeprint from humpback whale courtesy of Kuanyin Moi (left) Typical print from artificial fluke in process of forming (right).

There is currently not extensive research on the phenomenon of whale prints. Scientific literature prevalently attribute hydrodynamic forces, such as vortices, to flukeprints [2, 16]. At the same time, the glossy, slick-like appearance of the print and the fluid ridge at its edge is reminiscent of small oil slicks left by motorboats on the ocean surface. This has fueled popular theories that surfactants

(surface tension-reducing substances) have created the prints [5]. Surfactant gradients (changes in the concentration of surfactant on the surface of a liquid) are a mechanism for bio-locomotion of insects [28] and biofilms [1]. The surfactant facilitates locomotion because if the insect expels surfactant from the rear, then the surface tension ahead of the insect is higher, and the surface will pull the insect forwards. Likewise, surface spreading due to surfactants can create smooth patches such as those of the flukeprints. This "calming of the waters" by surfactants such as oil or soap has been known since ancient times [15].

Marine biologists note that there are several reasons that surfactants might be present in the whaleprints. One hypothesis concerns the whale's oily skin, which could act as a sufactant. Cetaceans (whales, porpoises and dophins) shed their oily skin at approximately fifty times the rate of humans [27]. The skin is usually exfoliated during social activities such as lobtailing and breaching [18], and skin fragments can subsequently be found in the whale's flukeprints. Although researchers regularly collect skin samples from the flukeprints, the material is sparse and not always evident. Therefore, the volume of skin sloughed is unlikely to be large enough to cause a significant surfactant effect.

Another hypothesis concerns algae brought to the surface by fluke motion. The algae may release surfactants and may cause the flukeprints to appear [22]. Yet another hypothesis is that the remains of feeding could be left on the surface as the whale dives, leaving a print behind as the contaminants act as a surfactant. While these effects could be present, the evidence is not compelling as the primary origin of the prints.

In contrast, observations by marine biologists at Cascadia Research provide strong evidence that hydrodynamics are the primary mechanism for print formation. The researchers film blue whales above and underwater at close range by approaching the whales in small boats. The first observation is that a buoyant object (such as an orange) thrown into a flukeprint consistently moves to the outer edge of the print. This indicates that there is steady movement of water from the center of the print to the edge. Since this movement occurs at a range of times that the print is visible and not just during the formation of the print, the motion is unlikely to be caused by a gradient in surfactant concentration, which would die out as the concentration rapidly equilibrates.

The second observation is in video footage of vortices being shed from a blue whale fluke as the whale begins a terminal dive. The upward thrust of water from the motion of the fluke is visible due to particulate matter in the ocean which acts as tracer particles. The motion indicates strong hydrodynamic forces originating below the surface when the whale is fluking during shallow swimming or just before a terminal dive. This is in contrast to the motion of the whale during a terminal dive, since the whales are negatively buoyant and do not need to fluke once they are headed down from the surface.

A final observation, notable in the photograph of Fig. 1, is that while small wavelength capillary waves are absent in the print, long wavelength waves are still evident. This is typical of whale flukeprints observed in the ocean. This phenomenon will be discussed and explained by related experiments described in the final section of the paper.

The observations indicate that the presence of surfactants is of secondary importance for the formation of flukeprints to hydrodynamics created by the fluke. The goal of this project is to create and analyze flukeprints made with an artificial fluke without the introduction of surfactants. This pilot study provides evidence that flukeprints are created primarily through hydrodynamics.

Materials and Methods

To create flukeprints, the researchers fabricated a polypropylene fluke (uniform thickness 0.09 in.) replicating that of a blue whale (*Balaenoptera musculus*) by creating a pattern from the photograph in Fig. 2. In cetaceans, the fluke planform has a tip-to-tip span ranging from 0.2 m (for porpoises) to 3.5 m (for whales) [3]. The fluke replica had fluke span, S (m), the lateral length from tip-to-tip of 1.05 and a mean chord length, C (m), the average between tip chord and root chord of 0.37.

The researcher stood in chest-deep water in an outdoor pool with length 23 m, width 14 m, and

depth > 1 m. Preliminary experiments were performed to determine the distance from the edge of the tank where the reflection of waves would create the least disturbance. To create prints, the researcher walked backwards with the hand-held fluke oscillating in a sinuisoidal trajectory in the dorsoventral plane.

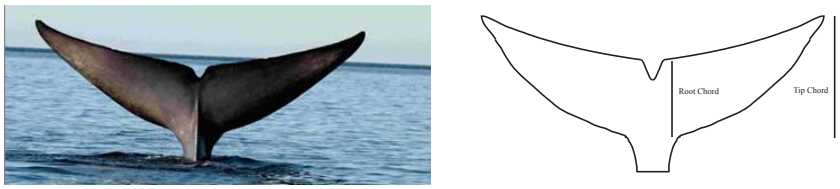

Figure 2: Fluke photograph courtesy of Students on Ice.

Cetacean locomotion makes use of the posterior one-third of the body to create dorsoventral movement of the fluke [9]. The flukes act as a hydrofoil for thrust and generate the necessary energy for propulsion [8, 12]. When the tail is at the top of its stroke, the fluke is horizontal and therefore minimizes drag. On the downward stroke, the fluke bends upward relative to the longitudinal axis (maximum at the middle of stroke), until the tail reaches the bottom of its stroke. At that point, the fluke is once again horizontal. On the upstroke, the fluke bends downward until the tail reaches the top of its stroke [21]. Such movement is characterized as a lift-based propulsion [10]. The angle of attack ranges from 12° to 20° for dolphins swimming at velocities ranging from 1.22 ms^{-1} to 6.0 ms^{-1} [9]. Whales can swim anywhere from 1.5 ms^{-1} to 8 ms^{-1} [11].

In the experiments, on the downstroke, the fluke was bent upward, relative to the horizontal line, with a downstroke angle of attack, $10° \pm 3°$ and pitch angle,30°.(deg). At the bottom and top of a stroke, the fluke flattened out to a horizontal level. Unlike that of a cetacean's movement [10], the fluke was bent upward on the upstroke with an upstroke angle of attack, $75° \pm 5°$, and pitch angle, $25° \pm 5°$ (see Fig. 3). The fluke started approximately 0.15 m below the surface, dropped 0.20 m $\pm$ 0.1 m and returned to 0.15 m below surface in a sinuisoidal trajectory with a wavelength of 1.0 m $\pm$ 0.1 m.

A video camera was used to collect data from seventy one trials. Data from 67 of the trials were retained; the other points were outliers. Recordings of the experiments were then replayed in the lab, on a 21″ monitor and translational time and flukeprint data (width, length and duration) were retrieved. 5″ reference markings on the model fluke allowed the researchers to scale the monitor's aspect ratio to its true proportions. Swimming velocity, (U, ms^{-1}), was calculated by recording the time taken to travel a translational distance comprised of four complete oscillations. Footprint width, length and duration were also recorded.

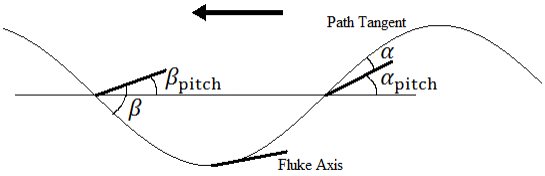

Figure 3: The angle of attack was measured as the angle between the fluke axis and path tangent [9]. The pitch angle is the angle between the tangent of the chordwise plane of the fluke and the axis of forward progression [11]. The downstroke angle of attack, α, was $10° \pm 3°$ and the pitch angle, α_{pitch}, was 30°. The upstroke angle of attack, β, was $75° \pm 5°$ and the pitch angle, β_{pitch}, was $25° \pm 5°$. The error is due to the lack of precision of motion.

Experiments were also performed a) without the researcher moving, b) with upstroke first then downstroke movement (see Fig. 3) and c) at a different starting depth and amplitude. However,

a downstroke-upstroke during translational movement produced flukeprints with the most clearly defined print boundary.

Experimental Trials

The experiments were organized into seventy one trials consisting of four successive sinuisoidal oscillations with an amplitude, A, of 0.2 m $\pm$ 0.1 m and a wavelength of 1.0 m $\pm$ 0.08 m. During each independent trial, the length, width and duration of the first flukeprint was recorded, since the subsequent flukeprints sometimes overlapped. Furthermore, of the first flukeprints, only the clear flukeprints were recorded.

Table 1: Swim Velocity

Swim velocity (ms^{-1})	Error (ms^{-1})	Number of points (n)
$0.33(0.31 - 0.36)$	0.04	19
$0.39(0.37 - 0.42)$	0.03	24
$0.49(0.46 - 0.51)$	0.03	10
$0.54(0.52 - 0.55)$	0.03	11
$0.60(0.57 - 0.65)$	0.04	7

Swim velocities are means with the range given in parenthesis. Number of measurements n are given in the third column.

The seventy one trials were conducted at a wide range of swim velocities, from 0.25 ms^{-1} to 0.65 ms^{-1}. The velocities were determined after from the video and then clustered (see Table 1). Larger velocities caused too much bending of the fluke, a trend evident in the data of Figure 4. For velocities $U < 0.35$ ms^{-1}, no flukeprints were measured because they were not clear enough to be measured.

A typical experimental flukeprint had an elliptical shape with a ragged contour but a well-defined boundary marked by ridges in the water. An average flukeprint was 0.75 m wide (measured along the minor axis) by 1.00 m long (measured along the major axis). The widths varied from 0.35 m to 0.95 m and the lengths varied from 0.70 m to 1.5 m. The duration of the prints ranged from four to seven seconds. If there was uncertainty on whether or not a flukeprint formed, the flukeprint was not included in the data.

Flow Characterization

To determine that the motion creating the prints in the experiments is plausibly similar to that of Cetaceans, two non-dimensional numbers, the Strouhal and Reynolds numbers, are used to characterize the flow. The Strouhal number, often used to characterize the motion of swimming and flying, is the ratio

$$St = \frac{Af}{U} \tag{1}$$

where A (m) is the amplitude of each stroke, f (Hz) is the frequency of vortex shedding and U is the velocity in the horizontal direction [29]. Swimming and flying animals generally move with Strouhal numbers in the range $0.2 < St < 0.4$ regardless of the size of the animal or the fluid medium (air or water) [26]. The Strouhal numbers for the experiments of this paper, detailed in Table 3, were within this range, and close to the Strouhal number of 0.25

A second nondimensional number characterizing the flow, the Reynolds number

$$Re = \frac{UC}{\nu} \tag{2}$$

quantifies the relative effect of viscous and inertial forces acting on the medium. Here U, (ms^{-1}) is the swimming velocity, C (m) is the mean chord length and ν is the kinematic viscosity of water, 20° (1.0×10^{-6} $\mathrm{m}^2\mathrm{s}^{-1}$). Low Reynolds numbers are characteristic of slow, viscous flows, such as honey, whereas high Reynolds number flows are typical of turbulent flows, such as the air flow over the wing of an airplane. Since video of blue whales taken underwater by divers with Cascadia Research contain evidence of vortices below the surface created by the oscillation of the flukes, a Reynolds number consistent with vortex shedding was desirable in the experiments.

For the seventy one experimental trials, after the swimming velocities were recorded and clustered, the Reynolds and Strouhal numbers were calculated for each cluster (see Table 2). Six different values for Reynolds and Strouhal numbers were obtained. The range of Reynolds number is below that what was expected for cetacean swimming ($10^6 - 10^7$) [9, 17]. The large Reynolds number, however, is within an appropriate range for vortex formation [29]. The small Strouhal number remained the same throughout the experiment, as expected, and was consistent with values for cetacean fluke locomotion.

Table 2: Reynolds and Strouhal numbers

Swim velocity (ms^{-1})	Reynolds Number	Strouhal Number
$0.33(0.31 - 0.36)$	124529 ± 6000	0.21 ± 0.08
$0.39(0.37 - 0.42)$	146123 ± 5600	0.20 ± 0.08
$0.49(0.46 - 0.51)$	184324 ± 5400	0.20 ± 0.08
$0.54(0.52 - 0.54)$	199990 ± 3400	0.21 ± 0.08
$0.60(0.57 - 0.63)$	223315 ± 10000	0.20 ± 0.08

Error given for Strouhal number is calculated using the uncertainty and standard deviation added in quadrature. Number in parenthesis is a range of swim speeds for each category.

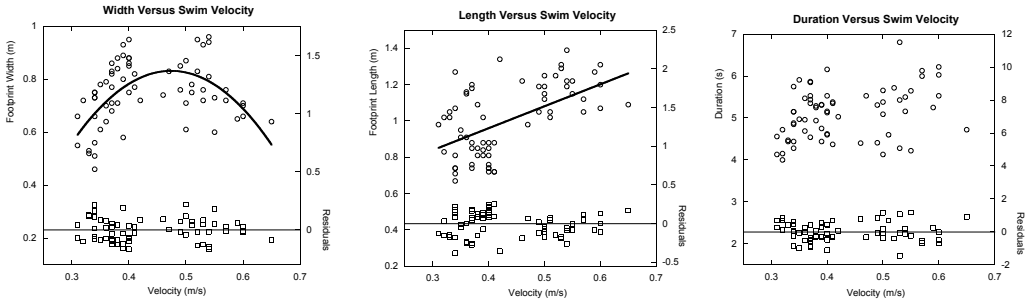

Figure 4: Relationship between the width of a flukeprint, w (m), the length of a flukeprint, l (m), the duration of flukeprint and swim velocity, U (ms^{-1}). $n = 67$ for each graph. The dimensions of measureable flukeprints were taken approximately 3 seconds after the flukeprint's formation (Average duration of flukeprint was about 5 sec). The data was split into six categories, grouped according to velocity. It was then weighed by calculating the standard deviation of each point from its respective average. Bottom panels show residuals that appear to be random. No correlation is present between duration and swim velocity.

The horizontal velocity of the researcher and the frequency of the oscillations were positively correlated, with a regression coefficient of $R^2 = 0.97$. This indicates that the researcher was moving in a consistent fashion in terms of how much oscillation was imposed for a given velocity. This consistency of movement could be related to the narrow range of Strouhal number observed in nature.

Width, Length, and Duration of Flukeprint Versus Swim Velocity

During each trial, the width and length as well as the duration of the flukeprint were recorded. Each statistic is compared to swim velocity in Fig. 4, which contains scatterplots and fitted curves for the results of the trials as well as residual plots at the bottom. Four outliers were removed from each plot based on the residuals. While there was much scatter in the data, some general trends were observed. The relationship between velocity and width appeared parabolic (regression coefficient $R^2 = 0.35$), while the relationship between velocity and length appeared linear ($R^2 = 0.25$). While the R^2 values may seem low, they are typical for biological experiments in which there is a great dal of variation expected between trials. No relationship between velocity and duration could be deduced.

The difference in results for width and length of flukeprints can be explained by the material properties of the fluke. As more force was applied to the polypropylene fluke to increase the velocity and frequency, the fluke bent in the direction perpendicular to the motion but not in the direction of the motion. Thus for low velocities, the fluke exerted less force on the water and created small width prints. As the velocity increased, the print width became larger until the bending began to decrease the size of the prints. This led to the generally parabolic shape of the width data. In contrast, as the velocity increased, the length of the flukeprints increased monotonically as the distance traveled during one cycle and the force exerted on the fluke increased.

Table 3: Flukeprint Width, Length and Duration Statistics

Dimension	Regression Equation	R^2
Width	$w = -1.19 + 8.52U - 8.99U^2$	0.349
Length	$l = 0.48 + 1.21U$	0.252

Amplitude and Depth

All of the experiments described above were conducted at a starting depth of 0.15 ± 0.05 m and an amplitude of 0.2 m. To investigate the effect of amplitude and depth on the prints, two additional experiments were performed (ten trials each). The first experiment, run at $U = 0.45$ ms^{-1} $\pm$ 0.05 ms^{-1}, had the original amplitude (0.2 m) but a different initial depth: 0.3 ± 0.05 m. The second experiment, run at $U = 0.4$ ms^{-1} $\pm$ 0.05 ms^{-1}, had the original depth (0.15 ± 0.05 m) but a different amplitude: 0.65 ± 0.05 m. A delay was observed in the formation of flukeprints for the deeper initial position. The prints from the experiment with the larger amplitude were smaller in length and width.

Discussion of related experiments

While the experimental results provide evidence for the formation of flukeprints without surfactants, previous experiments provide evidence for the characteristically smooth patch that makes the prints so visually striking in the ocean. In two papers from the 1955 Proceedings of the Royal Society A, Sir G. I. Taylor and Prof. J. T. Evans [6, 25] discuss an experiment in which bubbles released from the bottom of a tank create an upwelling of current which disrupts surface waves. The surface waves were generated to mimic wind-driven capillary waves that might be found in a ship harbor. The papers contain theory developed to find a mechanism for reducing wave action in ocean harbors.

The papers contain a set of calculations for the maximum wavelength of surface wave that can be disrupted by a current of given velocity. The wavelength is a function of the current velocity and the frequency of the wave to be disrupted. The same formulae can be inverted to instead calculate

the speed at which the current must flow to stop waves of a given length. The papers demonstrate that while waves can be disrupted by a horizontal current initiated by a vertical jet of fluid, that for reasonable current velocities, only the shorter wavelengths would be eradicated.

Unfortunately, since the long wavelengths were of concern in the harbors, the mechanism was not deemed viable for the protection of ships. However, the relationship, confirmed by Taylor and Evans in experiments, provides a viable explanation why long wavelength patterns are visible in flukeprints, while smaller wavelengths are disrupted. The fluid sent to the ocean surface by the fluke, once at the surface, travels out horizontally from the center of the print, creating an effect analogous to the currents Taylor and Evans produced with a jet of fluid or with a stream of bubbles. The outward current disrupts the small wavelength wind-driven capillary waves leaving a visibly smooth path containing only long wavelength oscillations such as those in the photograph of Figure 1.

Another explanation for the disruption of capillary waves is that the water in the jet displaces the water formerly at the surface, and in this new patch of water, capillary waves have not had time to form. Concurrent with this research, a study was conducted on the thermal properties of the whale prints of a female humpback whale [4]. Flukeprints were photographed from the air using an infrared camera. The flukeprints were visible because the temperature in the prints was less than that of the ocean surface temperature. The researchers modeled the difference in temperature between the nearby sea surface temperature and the temperature at the center of the flukes. Using a simple hydrodynamic model in which a jet of water the width of the fluke mixes turbulently with the surface water, the cooling of the water in the print is described using an exponential function. The measurable difference in surface temperatures inside and outside the flukeprint further support the theory that the prints are created as the motion of the flukes brings water to the surface of the ocean.

While a simple jet may be forming the print, another explanation is suggested by the three-dimensional numerical simulations that compare the vorticity shed during the swimming of dolphins and humans (performing a dolphin kick) [19]. In these simulations a vortex rings are shed on the up and down strokes. On the upstroke, the ring travels upward and then dissipates. The simulations do not have interaction with a surface, but if the circulation is the correct direction, it could explain the movement of the orange thrown into the print that moves to the outer edge, even after the print is formed.

Conclusions

The researchers were able to demonstrate that clear flukeprints can be formed from hydrodynamic forces without the use of surfactants. The conclusions drawn from the experiments with an artificial fluke are reinforced by observations of the fluid movement and temperature in authentic whale flukeprints, mathematical models and numerical simulations. This preliminary investigation indicates that flukeprint length and width increase monotonically with swim velocity, until the bending of the fluke reduces the width of the print. In this study the duration of the print did not appear to be related to swim velocity while the time to formation is increased by the depth of the fluke.

The investigations of this paper indicate a need for more controlled studies of surface response to fluke motion. Work currently in progress will employ robotic flukes to provide more controlled studies of fluid-structure-surface interactions. These experiments will provide data collected after varying a number of parameters, such as depth, frequency of oscillation, forward velocity and fluke shape. By varying the inclination angle, we can compare the footprints made by horizontal cruising motions to those of a terminal dive. Future results will be compared to video of whale movement above and below the ocean surface, data from motion sensors places on the whales, and numerical simulations of vorticity as it interacts with a fluid-air interface.

Acknowledgements

We would like to thank Dr. Catherine McFadden of the Biology department and Lori Bassman of the Engineering department at Harvey Mudd College. We would like to thank Ann Bowles of Hubbs-Sea World Research Institute, Marshall Tulin and Ivo Ros for helpful discussions. This research was supported in part by funds from the Harvey Mudd College Center for Environmental Research.

References

[1] Angelini, T.E., Roper, M., Kolter, R., Weitz, D., Brenner, M. (2009). Bacillus subtilis spreads by surng on waves of surfactant. *Preprint*.

[2] Baker, A.N. and Madon, B.(2007). Brydes whales (*Balaenoptera* cf. *brydei* Olsen 1913) in the Hauraki Gulf and northeastern New Zealand waters. *Science for conservation*. **272**,1-14. Retrieved July 2.

[3] Bose N., Lien J. and Ahia J.(1990). Measurements of the Bodies and Flukes of Several Cetacean Species. *Proceedings: Biological Sciences*. **242, No. 1305**, 163-173. Retrieved August 15.

[4] Churnside, J., Ostrovsky and Veenstra, T. (2009). Thermal Footprints of Whales. Oceanography. **22**, 206-209.

[5] downundergal. (2007). Whale Footprints. From *http://www.globosapiens.net/downundergal/picture-whale-footprint-24956.html*. Retrieved May 29, 2008.

[6] Evans, J.T. (1955) Pneumatic and Similar Breakwaters. Proc. R. Soc. Lond. A, **231**,457-466.

[7] Felts, W.J.L. (1966). Some Functional and Structural Characteristics of Cetacean Flippers and Flukes. In *Whales, Dolphins and Porpoises*. pp. 255 - 276. University of California Press. Retrieved July 2.

[8] Fish, F.E. and Hui, C.A. (1991). Dolphin Swimming - a Review . *Mammal Rev.*. **21, No. 4**, 179-193. Retrieved July 1.

[9] Fish, F.E. (1993b). Power Output and Propulsive Efficiency of Swimming Bottlenose Dolphins (*Tursiops truncatus*). *J. Exp. Biol.*. **185**, 179-193. Retrieved July 1.

[10] Fish, F.E. (1996). Transitions from Drag-based to Lift-based Propulsion in Mammalian Swimming. *Amer. Zool.*. **36**, 628-641. Retrieved July 15.

[11] Fish, F.E. (1998). Comparative Kinematics and Hydrodynamics of Odontocete Cetaceans: Morphological and Ecological Correlates with Swimming Performance. In *J. Exp. Biol.*. **201**, 2867-2877. Retrieved July 2.

[12] Fish, F.E. and Rohr, J.J. (1999). Review of Dolphin Hydrodynamics and Swimming Performance. *Technical Report*. **1801**, 1-193. Retrieved July 2.

[13] Forslind, B. and Lindberg, M. (2004). Skin, Hair, and Nails: Structure and Function. *Informa Health Care*. pp. 206.

[14] Hacking. (2008). Marine Mammals. From *www.hackingfamily.com/images/Footprint_C_M.jpg*. Retrieved June 11, 2008.

[15] Huhnerfuss, H. (2006). Oil on Troubled Waters – A historical survey. Marine Surface Films, Springer-Verlag, 3-12.

[16] Lang, A.W. and Thacker, W.D. (2008). On the Interaction of Water Waves With a Surface-Parallel Vortex. *J. Flui. Engr.*. **130**, 051302-1 - 051302-1.

[17] Lighthill, M.J. (1969). Hydromechanics of Aquatic Animal Propulsion. *Annu. Rev. Fluid.* **1**, 414-446.

[18] Mann, J., Connor R.C., Tyack P.L., Whitehead, H.(2000). Cetacean societies: field studies of dolphins and whales. *University of Chicago Press*. pp. 82.

[19] Mittal, R., Mark, R. and Hahn, J. Full Body Analysis of Swimming Techniques. From *http://project.seas.gwu.edu/ fsagmae/Swim*. Retrieved March 26, 2009.

[20] oceanspot. (2007). View of Blue Whale's Blowholes and Whale 'Footprints' . From *www.youtube.com/watch?v=UiBqfg1b7CA*. Retrieved May 29, 2009.

[21] Parry, D.A. (1949). The Swimming of Whales and a Discussion of Gray's Paradox. *J. Exp. Biol.*. **26**, 24-28.

[22] Parshikova, T.V. (2003). Involvement of Surfactants in the Regulation of the Development of Microscopic Algae. *Hydrobiological Journal/Gidrobiologicheskiy Zhurnal* **39** [np].

[23] Scammon, C.M. (1968). The Marine Mammals of the North-western Coast of North America. *Dover Publications*. pp. 17.

[24] Sundown. (2008). Whale Watching Kauai. From *www.whale-watching-kauai.com*. Retrieved May 29, 2008.

[25] Taylor, G.I. (1955). The Action of a Surface Current Used as a Breakwater. Proc. R. Soc. Lond. A **231**, 466-478.

[26] Taylor, G.K., Nudds, R.L. and Thomas, A.L.R.(2003). Flying and swimming animals cruise at a Strouhal number tuned for high power efficiency. *Nature*. **425**, 707-710.

[27] Valsecchi, E., Glockner-Ferrari, D., Ferrari,M., Amos, W. (1998). Molecular analysis of the efficiency of sloughed skin sampling in whale population genetics. *Molecular Ecology*. **7, No. 10**, 1419-1422.

[28] Kevina Vulinec (9187). Swimming in Whirligig Beetles (Coleoptera: Gyrinidae): A Possible Role of the Pygidial Gland Secretion, *The Coleopterists Bulletin*, **41**, 151-153.

[29] Vogel, S.(2003). Comparative Biomechanics: Life's Physical World. pp. 282 and pp.128.

[30] Whitehead, H. (2003) Sperm Whales: Social Evolution in the Ocean. *University of Chicago Press*. pp. 83.